New Horizons in Earth Reinforcement – Otani, Miyata & Mukunoki (eds)
© 2008 Taylor & Francis Group, London, ISBN 978-0-415-45775-0

Rainfall seepage analysis and dynamic response analysis for the railway embankments seriously damaged in the 2004 Niigata-ken Chuetsu earthquake

T. Matsumaru, M. Tateyama, K. Kojima, K. Watanabe & M. Shinoda
Railway Technical Research Institute, Tokyo, Japan

M. Ishizuka
Integrated Geotechnology Institute Limited, Tokyo, Japan

ABSTRACT: Due to the 2004 Nigata-ken Chuetsu earthquake, a lot of fill structures and retaining walls collapsed. It seems that strength of fill structures was loosed because of rainfall induced by typhoon before this earthquake. So, using a set of numerical analyses, we evaluated correlation between rainfall and earthquake in the damages of a fill structure. In this paper, we introduce the outline of the collapsed fill, methods of numerical analyses, and the results of seepage analysis and dynamic response analysis. We chose the fill in the vicinity Jouetsu Line 221 km000 m. This fill was damaged severely and reconstructed with reinforced soil. From the seepage analysis, it revealed that moisture-content state of the collapsed embankment increased before the earthquake and rainwater drainage of the reconstructed embankment improved. Moreover, from the dynamic response analysis, it was clearly shown that the seismic stability of the restored embankments was significantly improved as compared to that of the damaged embankment by evaluating the response accelerations and deformation of the damaged and restored embankment.

1 INTRODUCTION

The 2004 Nigata-ken Chuetsu earthquake caused wide-spread area damages of fill structures and retaining walls. In railway field, 86 soil structures collapsed at the Jouetsu Line, the Shinetsu Line, the Iiyama Line and the Tadami Line (Tateyama and Kato, 2005). A lot of damages of soil structures occurred on the river terrace and overlap the places where sediment disasters induced by rainfall have occurred. Nigata Prefecture was affected by the rainfall of typhoon No.23 just before this earthquake, so it seems that the main reason of these damages are the decrease of strength with the increase of the degree of saturation in embankments. But the precise estimation has not been conducted.

In this paper, a set of numerical simulations aimed at the embankment in the vicinity Jouetsu Line 221 km000 m are conducted to evaluate the main reason of damage and the seismic resistance of the reconstructed embankment. First, an outline is given for the damaged embankment and the reconstructed embankment. Then, methods of seepage analysis, dynamic response analysis and deformation analysis by Newmark's method are introduced briefly. Finally, we show the results of seepage analysis and dynamic response analysis. The results of deformation analysis by Newmark's method are shown in Shinoda et al. (2007).

2 OUTLINE OF DAMAGED EMBANKMENT AND RECONSTRUTED EMBANKMENT

2.1 *Damaged embankment*

In the vicinity Jouetsu Line 221 km000 m, the embankment on the river terrace by the Shinano River collapsed. The damaged area was about 65 m long and 4 to 12 m high. The amount of collapsed soil was estimated to about 13,000 m^3. Figure 1 shows the illustration of damaged embankment and Figure 2 shows the photograph. The location of this embankment is valley eroded by the Shinano River. In this area, Route 17 runs alongside the Jouetsu Line, so the embankment of this route was also collapsed. The bedrock is sandy rock with middle particle and the silty rock accumulates on the bedrock. The material which consists of the damaged-embankment on the silty rock is sand with gravel.

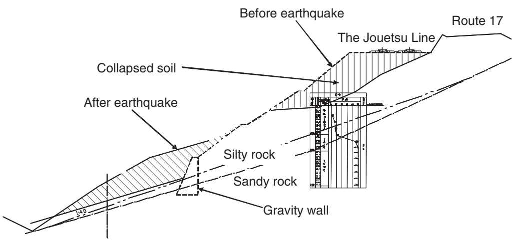

Figure 1. Illustration of damaged embankment.

Figure 2. Photograph of damaged embankment.

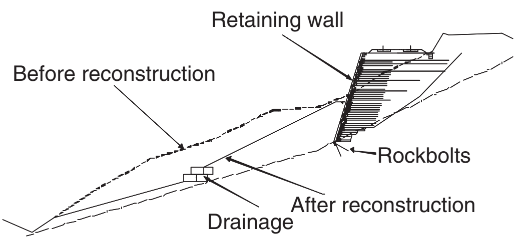

Figure 3. Illustration of reconstructed embankment.

2.2 *Reconstructed embankment*

The concept of reconstruction of the embankment was to reduce the amount of soil and days and to improve seismic resistance. Considering these conditions, geosynthetic-reinforced soil retaining wall was adopted. Figure 3 shows the illustration of reconstructed embankment and Figure 4 shows the photograph. Firstly, the collapsed soil was excavated until the silty rock. Before constructing the foundation of retaining wall, the rock bolts were installed in order to improve the stability of embankment. For the design of the reconstruction, load acting the road was also considered. The embankment was established until the height of 13 m with the geogrid every 30 cm. Furthermore, this embankment is located in drainage area and the boiling was observed after the earthquake.

Figure 4. Photograph of reconstructed embankment.

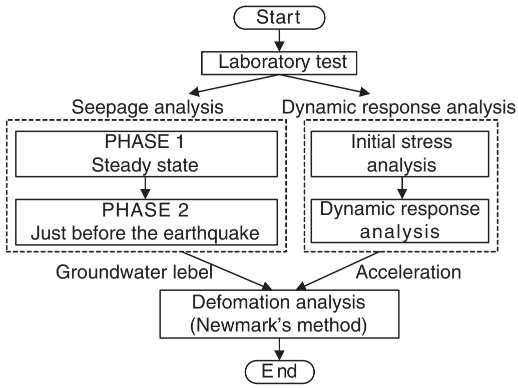

Figure 5. Flow of numerical simulations.

So, the improvement of drainage was also important. The amount of crushed stone used for reconstructing embankment was about 4,600 m^3 and concrete of RC wall was about 300 m^3.

3 OUTLINE OF NUMERICAL SIMULATIONS

In this section, we will show the outline of numerical simulations to evaluate the main reason of damage of embankment and the seismic improvement of reconstructed embankment. Figure 5 shows the flow of numerical simulations.

3.1 *Seepage analysis*

The degree of saturation in the damaged embankment may have increased because of the rainfall induced by typhoon No.23, so the drainage was important in the reconstructed embankment. We set the purpose of seepage analysis to evaluate the degree of saturation in the damaged embankment just before the earthquake and the improvement of drainage in the reconstructed embankment.

In this paper, the seepage analysis is conducted in two phases. In PHASE1, the seepage in the steady state is analyzed by using the rainfall for a long term equivalent to the annual rainfall. In PHASE2, the seepage just before the earthquake is analyzed by using the data observed at the site.

3.2 *Dynamic response analysis*

The purpose of the dynamic response analysis is to evaluate the response in the embankment subjected to the earthquake. In this analysis, after the initial stress is evaluated by the static analysis, the dynamic response is analyzed when the earthquake occurs in this stress state.

3.3 *Deformation analysis using Newmark's method*

The deformation of the embankment is analyzed by Newmark's method. In order to evaluate precisely the behavior in the earthquake, the response acceleration of the embankment acquired in the dynamic response analysis was considered. Furthermore, we take into consideration the strength parameters and the groundwater according to the degree of saturation seepage analysis. This part is introduced in the paper written by Shinoda et al. (2007).

4 SEEPAGE ANALYSIS

4.1 *Model of seepage characteristics*

In the seepage analysis, modeling the seepage characteristics of unsaturated soils is important. In this paper, we used the Van Genuchten model (1980) for the soil water characteristic curve. This model is often used in seepage analysis and generally described as

$$\Theta = \left[\frac{1}{1 + (\alpha h)^n} \right]^m \tag{1}$$

where, Θ is the relative water content, h is the suction, and α, n and m are parameters determined by laboratory tests. Using the moisture water content θ, the relative water content is written as

$$\Theta = \frac{\theta - \theta_r}{\theta_s - \theta_r} \tag{2}$$

where, θ_s is the saturated moisture water content and θ_r is the lower limit of the moisture water content. From equation (1), the unsaturated moisture water content is described as

$$K_r(\Theta) = \Theta^{1/2} \left\{ 1 - \left(1 - \Theta^{1/m} \right)^m \right\}^2 \tag{3}$$

Table 1. Parameters of sandy loam.

θr	θs	α(1/cm)	m	n
0.065	0.41	0.075	0.471	0.5

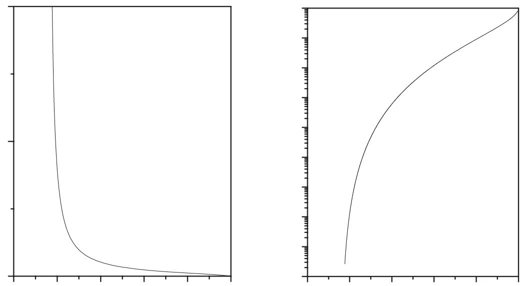

Figure 6. Relationship of the degree of saturation to the relative hydraulic conductivity and the suction.

where $K_r(\Theta)$ is the relative hydraulic conductivity, the ratio of the unsaturated hydraulic conductivity to the saturated conductivity.

As a usual, parameters in equation (1) are determined in the trial and error so that this equation describes the soil water characteristic curve obtained from laboratory tests. But, the laboratory tests of the collapsed soils were not conducted, so the parameters were determined according to the classification of soil characteristics in the standard of USDA (Carsel and Parrish, 1988). From this classification, all of the materials used in this analysis are classified as the sandy loam. Table 1 shows parameters of sandy loam, and Figure 6 shows the relationship of the degree of saturation to the relative hydraulic conductivity and the suction.

4.2 *Data of rainfall*

In this paper, seepage analysis is conducted in two phases. In PHASE1, the seepage in the embankment becomes in the steady state by using the annual rainfall, and in PHASE2 the degree of saturation just before the earthquake is analyzed by using the observed data of rainfall. Figure 7 shows the set of data of rainfall used in PHASE1 and PHASE2. The rainfall pattern in PHASE1 is 20.5 mm once every three days and 0 mm in the other days based on the annual average rainfall, 2500 mm in Nagaoka city. Using this rainfall pattern for 3,000 days, we have ensured that the degree of saturation in the embankment changes little. In PHASE2, the observed data of rainfall from September 1 until October 22 is used as the continual rainfall just before this earthquake.

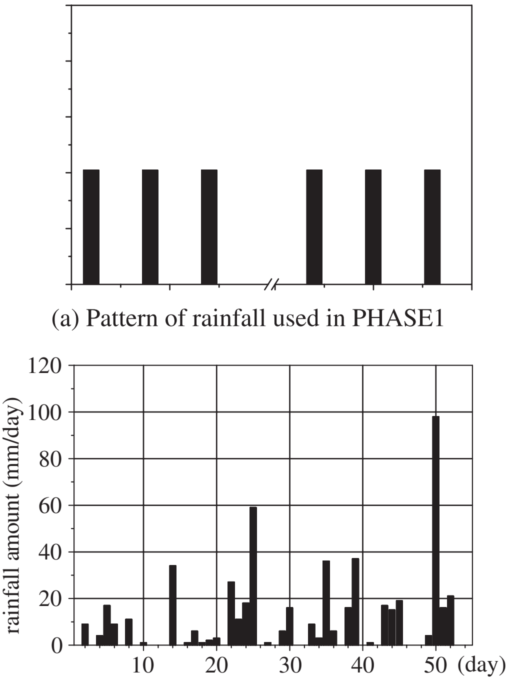

(a) Pattern of rainfall used in PHASE1

(b) From September 2004 until October 22

Figure 7. Set of data used in seepage analysis.

4.3 *Analytical conditions*

Figure 8 shows the analytical models. Both models consist of triangular elements, 31 m high by 90 m long. In these models, three materials; concrete, embankment material and weathering silt were considered. However, the concrete wall was not modeled as elements, but as the undrained boundary. From the situation of the damage, the rainfall just before the earthquake may have exceeded the capacity of the drainage, so the right edge was set under submerged condition. The hydraulic conductivity of the embankment 1.06×10^{-5}cm/s was determined from the laboratory test and conductivity of silty rock 1.00×10^{-3}cm/s was supposed from the comparison with the embankment material. Furthermore, the reconstructed embankment by crushed stone was also analyzed under the same rainfall. On the reconstruction, the drainage was improved, so the submerged condition was not considered. The hydraulic conductivity of the crushed stone 1.00×10^{-2}cm/s was supposed from the diameter.

4.4 *Results of analyses*

Figure 9 shows the distributions of degree of saturation in the embankment after the simulation in PHASE2. In the damaged embankment, the degree of saturation increases and the groundwater level appears along the boundary between the embankment and the silty rock. Though the capacity of the drainage in the embankment is not clear, the rainfall may exceed the capacity. So, this rainfall may have influenced the behavior of the embankment when the earthquake occurred. On the other hand, the degree of saturation in the reconstructed embankment was smaller than one in the damaged embankment. So, this indicates that the drainage in the reconstructed embankment was improved.

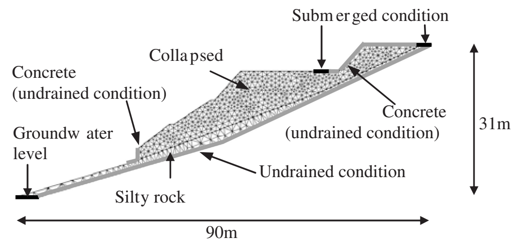

(a)Damaged embankment

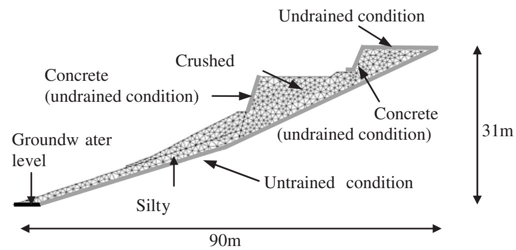

(b)Reconstructed embankment

Figure 8. Finite element models for seepage analysis.

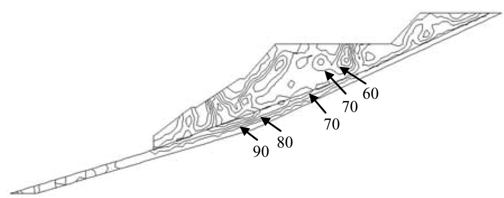

(a)Damaged embankment

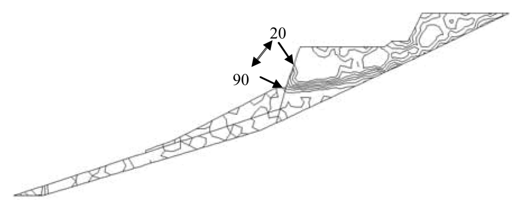

(b)Reconstructed embankment

Figure 9. Distributions of the degree of saturation (unit:%).

5 DYNAMIC RESPONSE ANALYSIS

5.1 *Modified GHE model*

In dynamic response analysis, modeling nonlinear characteristics of soil is important. R-O (Ramberg-Osgood) model or H-D (Hardin-Drnevich) model is often used because these models need not to determine a lot of parameters. But these models have difficulty of describing the relationship of shear strain to shear modulus and damping, from small-strain region to large-strain region. In this paper, modified GHE (General Hyperbolic Equation) model (Nishimura and Murono, 1999) as described in equation (4) is adopted. In this model, the hyperbolic model is applied to skeleton curve and Masing's rule is adopted to hysteresis curve. But as shown in equation (5) and (6), parameters C_1 and C_2 are modified to trace experimental results rather well.

$$\frac{\tau}{\tau_f} = \frac{\dfrac{\gamma}{\gamma_r}}{\dfrac{1}{C_1} + \dfrac{1}{C_2}\left(\dfrac{\gamma}{\gamma_r}\right)} \tag{4}$$

$$C_1(x) = \frac{C_1(0) + C_1(\infty)}{2} + \frac{C_1(0) - C_1(\infty)}{2} \cdot \cos\left\{\frac{\pi}{\alpha / x + 1}\right\} \tag{5}$$

$$C_2(x) = \frac{C_2(0) + C_2(\infty)}{2} + \frac{C_2(0) - C_2(\infty)}{2} \cdot \cos\left\{\frac{\pi}{\beta / x + 1}\right\} \tag{6}$$

where τ/τ_f is normalized shear stress, γ/γ_r is normalized shear strain, γ_r is standardized shear strain, defined by shear strength τ_f divided by initial shear modulus G_{max}, and $C_1(0), C_2(0), C_1(\infty), C_2(\infty), \alpha$ and β are parameters determined from laboratory tests. The equation which makes a correlation between damping factor h and shear strain γ is expressed by

$$h = h_{max}\left(1 - \left|\frac{\tau_a}{\gamma_a}\right| / G_0\right)^{\beta_{P6}} \tag{7}$$

where γ_a and τ_a are shear strain and shear stress at the turn-round point and β_{P6} is parameter.

5.2 *Analytical conditions*

Figure 10 shows the analytical models. In dynamic response analysis, we also compare the response of damaged embankment and reconstructed embankment. The damaged embankment consists of 1828 elements and 1848 nodal points, and the re-constructed embankment consists of 1705 elements and 1749 nodal points. For boundary conditions of deformation, all nodes at the bottom are fixed and the nodes at the right edge are fixed only in lateral direction. In dynamic response analysis, we modeled the sandy rock, silty rock, damaged-embankment material, reconstructed-embankment material and concrete. The modified GHE model was adopted for sandy rock, silty rock, embankment materials, and elastic model was adopted for concrete. Table 2 shows the input parameters and Figure 11 shows the dynamic deformation properties of sandy stone and reconstructed-embankment material using the parameters in Table 1. The modified GHE model describes

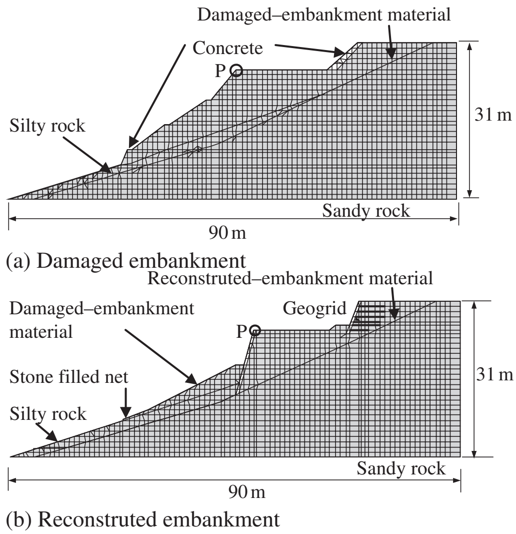

Figure 10. Analytical models for dynamic response analysis.

Table 2. Input parameters for ground, embankment and structure.

	Sandy rock	Silty rock and damaged-embankment material	Stone filled net and reconstructed embankment	Concrete
Shear modulus G_0(kPa)	830,000	30,275	338,679	1.04×10^7
Poisson's ratio ν	0.20	0.30	0.25	0.20
Cohesion c(kPa)	5.0	0.67	79.0	100.0
Internal friction angle ϕ (°)	49.0	33.63	47.8	0.0
Density ρ(t/m^3)	1.9	1.8	2.0	2.5
C1(0)	1.0	1.0	1.0	–
C2(0)	0.15	0.15	0.2	–
C1(∞)	0.2	0.1	0.2	–
C2(∞)	1.0	1.0	1.0	–
α	0.299	0.455	0.723	–
β	0.681	1.255	0.723	–
h_{max}	0.25	0.2	0.3	–
β_{p6}	1.1	1.5	0.08	–

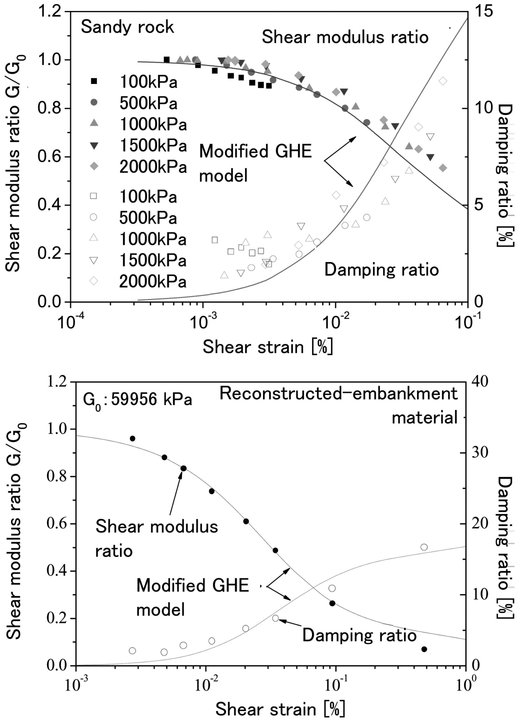

Figure 11. Dynamic deformation characteristics of sandy stone and reconstructed-embankment material.

Table 3. Input parameters for rock bolts and geogrid.

	Rock bolts	Geogrid
Young's modulus (kPa)	200,000,000	1,880,000
Moment of inertial (m^4)	1.17×10^{-8}	0.0002
Area (m^2)	9.60×10^{-5}	0.002

well dynamic characteristics obtained from laboratory tests. For reconstructed embankment, modeling the reinforcement materials is important. In this analysis, rock bolts and geogrid were modeled by beam elements and parameters of these materials were shown in Table 3.

The input wave is shown in Figure 12. This wave is inputted in horizontal direction.

5.3 *Results of analyses*

Figure 13 shows the distributions of maximum accelerations in the damaged embankment and the reconstructed embankment. In the damaged embankment, the maximum acceleration occurred at the top of slope. On the other hand, in the reconstructed embankment large acceleration occurred at the wide area. Figure 14

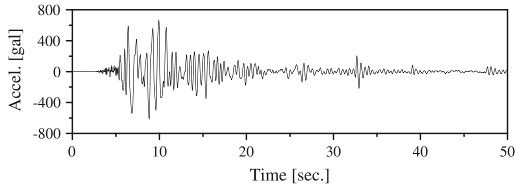

Figure 12. Input acceleration.

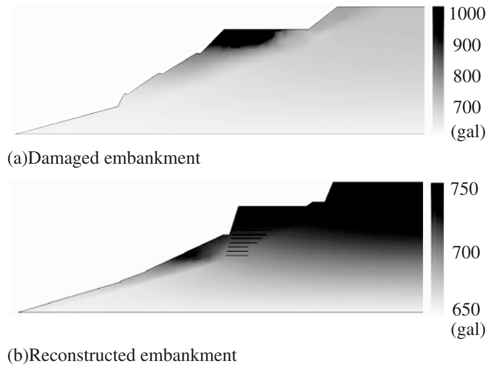

Figure 13. Distributions of maximum acceleration.

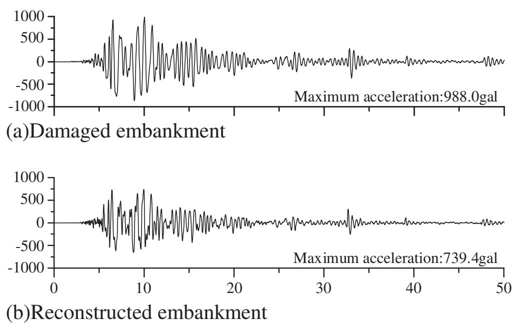

Figure 14. Time histories of acceleration at the top of embankment.

shows the time history of the accelerations at node P. The maximum acceleration in the reconstructed embankment was smaller than one in the damaged embankment. Figure 15 shows the deformation after this earthquake. The maximum lateral displacement of damaged embankment was about 10 cm, but that of the reconstructed embankment was very small. But the displacement obtained in the simulation of damaged embankment was considerably smaller than the observed displacement. From figure 15 (a), it is clear that a lot of finite elements at the top of embankment

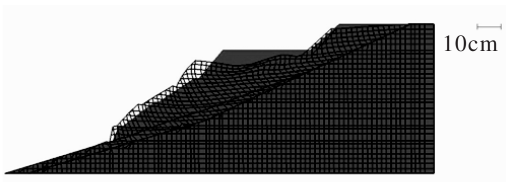

(a)Damaged embankment

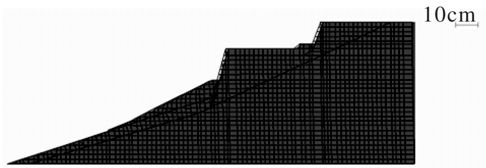

(b)Reconstructed embankment

Figure 15. Deformation after the earthquake.

were distorted. So, this indicates that this method has limitations for evaluating deformation.

6 CONCLUSIONS

In this paper, a set of numerical simulations were conducted in order to evaluate the main reason of collapse and the seismic resistance, aimed to the embankment in the vicinity Jouetsu Line 221 km000 m.

The seepage analysis provides the follow conclusions.

(1) In the damaged embankment, the degree of saturation increased and the groundwater level appeared along the boundary between the embankment and the silty rock.
(2) In the reconstructed embankment, the degree of saturation was smaller than one in the damaged embankment.

The dynamic response analysis provides the follow results.

(1) The maximum acceleration in the damaged embankment was larger than one in the reconstructed embankment. So, the seismic resistance of the reconstructed embankment was improved.
(2) The deformation obtained from the dynamic response analysis shows the same tendency of the maximum acceleration, but it revealed that the dynamic response analysis based on the FEM has the limitations to calculate the deformation of embankment.

According to the results obtained from the seepage analysis and dynamic response analysis, the deformation analysis using Newmark's method was conducted. The details are shown in Shinoda et al. (2007).

REFERENCES

Carsel, R. F. and Parrish, R. S. 1988. Developing joint probability distributions of soil water retention characteristics, Water Resources Research, No. 24, pp. 755–769

Nishimura, A. and Murono, Y. 1999. Proposal and experimental demonstration of nonlinear model of soil using the GHE model and the simple hysteretic rules, Proceedings of the JSCE Earthquake Engineering symposium, No. 29, pp. 309–312 (in Japanese)

Shinoda, M., Horii, K., Watanabe, K., Kojima, K. and Tateyama, M. 2007. Seismic stability of reinforced soil structure constructed after the mid Niigata prefecture earthquake, Proceedings of IS-Kyushu (submitted)

Tateyama, M. and Kato, S. 2005. Damages and lessons of railway structures in the 2004 Nigata-ken Chuetsu earthquake, the Foundation Engineering and Equipment, Vol. 33, No. 10, pp. 43–47 (in Japanese)

Van Genuchten, M. Th. 1980. A closed-form equation for predicting the hydraulic conductivity of unsaturated soils. Soil Sci. Soc. Am. J., No. 44, pp. 892–898